Journal of Proton Therapy
ISSN 2469-5491
www.protonjournal.org

Impact of the high magnetic field and RF power in a superconducting cyclotron on the operation of a nearby MRI facility

Chee-Wai Cheng[1], Steven G Ferguson[2], David Jordan[3], Frederick Jesseph[1], Mark Johnson[4], Lionel Bouchet[4], David Mansur[1], Barry Wessels[5]

[1] Department Radiation Oncology, University Hospitals Cleveland Medical Center, Cleveland, Ohio, USA
[2]Engineering Technical Services, Washington Laboratories, LTD, Gaithersburg, Maryland, USA
[3]Radiology, University Hospitals Cleveland Medical Center, Cleveland, Ohio, USA
[4]Mevion Medical Systems, Littleton, MA, USA
[5]Department of Radiation Oncology, Case Western Reserve University, Cleveland, OH, USA

Article history:
Submission: July 22, 2016
Revision: December 9, 2016
Acceptance: December 9, 2016
Publication: December 28, 2016

© Cheng. Published by EJourPub.

Cite this article as:
Cheng CW, Ferguson SG, Jordan D, Jesseph F, Johnson M, Bouchet L, Mansur D, Wessels B. Impact of the high magnetic field and RF power in a superconducting cyclotron on the operation of a nearby MRI facility. *Jour Proton Ther.* 2016; 2:213. DOI: 10.14319/jpt.21.3

Corresponding author:
Chee-Wai Cheng, PhD; Department Radiation Oncology, University Hospitals Cleveland Medical Center, Cleveland, Ohio, USA.

Abstract

The purpose of this study is to investigate whether the 9T superconducting magnet (9TSM) and the 11kW RF source in the Mevion S250 proton therapy system (S250PTS) produce interference in a nearby MRI facility. The RF shielding of the University Hospitals Proton Therapy Center (UHPTC) was designed by one of the authors (S. Ferguson) of Washington Laboratories Ltd., Gaithersburg, MD. A preliminary test was conducted to assess the effect of an external magnetic field on MR imaging. A time-varying magnetic field of 60G (more than 100 times the expected variance from the Mevion S250 9TSM) was generated (to simulate a rotating magnetic field) in the walkway between the nearest MRI suite (MR5) and the UHPTC (wall-to-wall distance 2.8 m) while scanning of a phantom was performed in MR5. The 9TSM was ramped up slowly and magnetic field testing was conducted at the 2T point and finally at the 9T level (full current at 1990 A). The 9TSM was rotated to different angles (0^o, 45^o, 90^o, 135^o, 180^o) while the magnetic field flux density was measured at different points inside the vault, in the walkway between the MR and UHPTC, and along the hallway inside the MR facility at each angle. The MR facility performed routine patient scanning on five clinical scanners throughout the 9TSM testing. With RF full power at 11 kW and the 9TSM rotated at different angles, the RF field strength was measured inside the vault and mid-point in the walkway (to evaluate the effectiveness of the RF shielding) and also between the two 3T MRI suites operating at 128 MHz center frequency where interference from the proton system RF emission would be a concern. Patient scanning was performed throughout the RF testing in all MRI suites. Finally, with the 9TSM at full current and RF full power, several phantom scans were performed in MR5 using MR scan sequences expected to be sensitive to time-varying magnetic fields and RF interference. No interference with MR imaging throughout the various RF and magnetic field testing was detected. This is the first report on interference of the strong time-varying magnetic field and RF power of the S250PTS in a nearby MRI facility. With proper RF shielding and site planning, the S250PTS may provide a viable solution to proton therapy in an urban setting where co-location is necessary or limited real estate restricts other installation options.

Keywords: Superconducting, Synchrocyclotron, Magnetic interference, RF interference, RF shielding

Original Article

1. Introduction

The University Hospitals Cleveland Medical Center in Cleveland, Ohio, decided in 2011 to add proton therapy to its existing radiation therapy equipment in order to provide broader services to its cancer patient population. The Mevion S250 Proton Therapy System (PTS) was chosen for its compactness and state-of-art technology in a rotational superconducting cyclotron. Geographically, the PTS installation places the Mevion S250 at a distance of ~8 m to the north wall of the closest MRI suite (MR5) in the existing MRI facility. An aerial view of the PTC and the MRI building is shown in Figure 1. Isocenter-to-isocenter distance between the Mevion S250 and the MRI scanner in MR5 is just under 11 m.

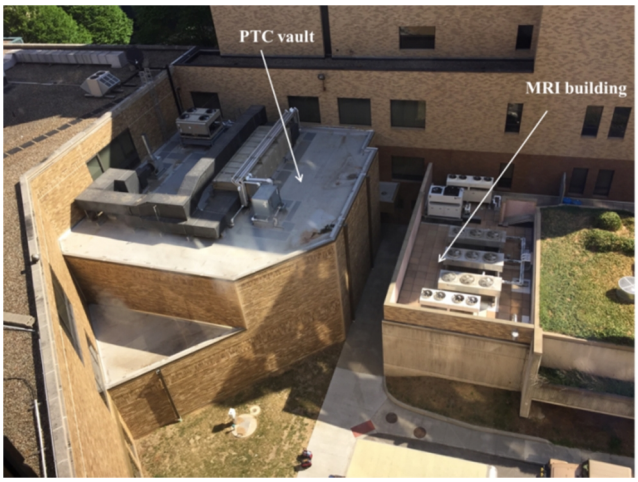

Figure 1: An aerial view of the UHPTC and the MRI buildings showing the proximity of the two constructions.

The Mevion S250 PTS combines proton accelerator and superconducting magnet technologies to form a compact proton therapy system that fits inside a single vault. The 9 Tesla (T) superconducting magnet (9TSM) together with an 11 kW variable-frequency (90-133 MHz) RF source produces a 250 MeV proton beam in a compact synchrocyclotron measuring 1.8 m in diameter and weighing 22.4 metric tons (22,400 kg).[1] The accelerator is surrounded by a magnetic shield[2] to reduce the footprint of stray magnetic field from the 9TSM. However, some amount of stray magnetic field remains and the flux lines emanating from the accelerator extend through space to surrounding areas. The synchrocyclotron is mounted on a gantry to provide isocentric proton therapy with coplanar and non-coplanar fields when coupled with a robotic couch (patient positioning system). As the gantry rotates from one angle to the next, the synchrocyclotron also rotates, producing an external time-varying magnetic field.

According to Faraday's Law of Induction, a time varying magnetic field (B) induces an electric current (eddy current) in a nearby stationary conductor. The eddy current in turn produces a magnetic field in the conductor that opposes the magnetic field that created it (Lenz's law). Both the magnitudes of the eddy current and the magnetic field it produces are proportional to the magnitude of the time-varying field B. Thus one of the major concerns with the Mevion S250 PTS is the generation of a time varying magnetic field due to gantry rotation, which may potentially interfere with imaging inside the nearby MRI department, particularly the nearest unit (labelled MR5), a 1.5T MRI scanner (Siemens Espree, Siemens Healthcare, Erlangen, Germany) (Figure 3). Calculations indicated that the risk of interference was low and that installation of a Magnetic Active Cancellation System (MACS) could mitigate the issue if present.

The 11 kW RF source in the synchrocyclotron operates in the 90-133 MHz frequency range, which overlaps with the RF operating frequency of the 3T MRI scanners (~128 MHz), located in MRI rooms 1 and 2. Each MRI suite is enclosed in an RF shield which rejects the stray RF signals outside the scan room. The RF shield can protect the MR scanner from interference of low-power RF from external sources. Although the Mevion system complies with international standards for RF emissions, peak RF emission level combined with the high RF sensitivity of the MRI scanners requires greater attenuation of such strong external RF signals, and the shielding provided for normal environmental background RF may not be sufficient for a powerful source such as the S250PTS sited in close proximity to the MR scanner.

In this paper, we report the design of the RF shielding for the Mevion S250 PTS, measurements within the MRI department of potential magnetic and RF interference sources designed to simulate the operation of the S250PTS, and measurements of MRI system performance and response to possible interference during operation of the S250PTS in its clinical operating configuration.

2. Materials and Methods

2.1. RF consideration

2.1.1. Shielding design

Prior to construction, RF measurements were performed to verify that the MRI facility provided appropriate RF shielding. Measurements were also carried out within the MRI facility using an external RF source at 123.5 MHz (the center frequency of the 3T MRI unit in Room 1) to determine the threshold where interference would produce artifacts in MR imaging. Interference in the MR images in MR1 was observed, indicating that there is a potential of RF interference to MR scanning of the Mevion S250 RF source. Thus RF shielding of the Mevion S250PTS must be provided to eliminate the interference to MR imaging.

To estimate the RF attenuation at distances from a Mevion

© Cheng et al. Published by EJourPub.

S250 accelerator, measurements were conducted at the Barnes Jewish Hospital (BJH) in St. Louis, which has a Mevion S250 PTS in clinical operation. Under beam-on condition (full power RF and full current in the superconducting magnet), measurements were taken at several points inside surrounding constructions at 'similar distances' of the UHPTC proton isocenter to MR5 isocenter. It should be pointed out that the term 'similar distances' is meant to be generalized distances in the BJH testing and not intended to be precise, but to provide an approximate basis of attenuation for the measurements at BJH. It was found that a total of 67 dB attenuation would be needed to ensure interference-free MR scanning. Approximately 7dB attenuation is needed to reach the incoherent threshold for the MR scanner, and ~60dB attenuation is needed for MRI coherent signal processing. It should be pointed out that the measurements performed at BJH also produced measurable magnetic field deviations at the measurement points due to the 9T magnet. These magnetic field strengths were later used as reference values in the magnetic field testing described in section 2.2.

A quick estimate of the existing RF shielding[3] at the MRI center indicated that: (1)10dB attenuation is provided by the North wall of the MRI facility; (2) 20dB is provided by distance from the Mevion S250PTS isocenter to the MR5 north wall; and (3) > 20dB is provided by the South wall of the proton center, (8' thickness with double rebar). Thus, shielding was required to provide at least 17dB additional attenuation. Since the overall RF interference may vary due to changing environmental sources and power levels, RF shielding was designed to provide at least 27dB attenuation to provide the needed control with a conservative margin.

2.1.2. RF Shielding construction

A screen mesh material attached to the rebar was chosen for RF shielding as most economical while providing the necessary RF attenuation. Two wire meshes connected by rebar rods and form-ties provide the RF shielding; the panels of one mesh overlap those in the second mesh to prevent gaps between overlapping panels and avoid separation due to future mechanical disturbance or thermal expansion. The mesh covers the entire south wall and extends to the northwest (NW) wall and the north wall (Figure 2, mesh outlined in red). The extension of the mesh to the northwest and east walls provides a means to reduce the potential refraction of RF toward the MRI facility. Grounding rods (red circles in Figure 1) placed along the perimeter of the shielded wall are connected together with copper wires placed below grade (the blue line in Figure 1), and the mesh screen shield is connected to the ground connecting wire. This secures the wire mesh below grade in the trench in the closed wall after pouring of concrete. Tungsten Inert Gas (TIG) welding was used to connect the ground wire to the ground rods to prevent corrosion from degrading the connection. Throughout construction, physical inspections and testing of installed parts were carried out to identify performance issues so that any needed corrective measures could be identified early. As an example, form-ties used to connect the two wire meshes were found to have penetrated the outer mesh, which would act as antennas of RF. Upon discovery, the form-ties were provided terminations to integrate them into the shielding, mitigating the risk of re-radiation by their penetrations. Thus early identification provided the opportunity to mitigate the issue prior to build completion so more options to compensate were available. The double wire mesh design provides over 60dB of reflected shielding effectiveness given its placement in the wall at more than 10 meters from the S250PTS RF source. The 60dB effectiveness was selected to provide a margin compensating for construction imperfections reducing the effectiveness. This exceeds the design goal of 27dB, providing additional margin for the overall design.

2.1.3. RF measurements

With RF full power at 11 kW, the RF field strengths were measured at different points (Figure 3) for different magnet angles (inset of Figure 3) at full current in the walkway between the PTC south wall and MRI North wall. RF field strengths were also measured at various magnet rotations at the entry of the equipment room (R3) located between MR1 and MR2 as the largest RF interference to MR scanning in MR1 was detected in an earlier measurement with a simulated RF field at 123.5 MHz as described in section 2.1.1 above.

2.2. Magnetic field consideration

2.2.1. Preliminary tests

Preliminary measurements were first conducted to establish the test levels and to assess free space attenuation of magnetic field on the Washington Laboratories Open Area Test Site. Two measurements were used to obtain the results. The first method used a triaxial Gauss meter with 10 mG sensitivity. The second method used a magnetic compass with a resolution of 0.1-degree and 0.3 mG sensitivity to detect interference signals at greater distances from the source. The horizontal magnitude of the Earth's magnetic field at the test site was obtained from the National Oceanic and Atmospheric Administration (NOAA) field calculator and used as the reference for compass variance.

2.2.2. Magnetic field measurements with a time-varying 60G field

Before the installation of the S250PTS, the effect of a time-varying magnetic field on MR imaging in the MRI facility was studied. A field coil measuring 1.5 meter in diameter (120 turns of wire driven by a 1600 Watt power amplifier at a frequency of 100 mHz), was used to generate a time-varying magnetic field similar to that produced by the S250PTS during gantry movement. The coil was placed outside of the north wall of MR5 (Figure 4). The signal source and amplifier setting were adjusted to produce a 60

© Cheng et al. Published by EJourPub.

G field at the coil. This magnetic field strength is more than 100 times the measured magnetic flux at BJH at the same distance under full current condition in the 9TSM. This very large magnetic field was chosen as the initial condition to provide a conservative margin. If a 60 G field did not produce interference to MR imaging on the nearest scanner, no further testing would be needed. Should the 60 G field produce interference to MR imaging, the field strength would be reduced sequentially and the testing is repeated. This approach was intended to minimize the amount of MRI scanner time needed to determine the interference threshold.

Prior to creating an interference signal in the coil, an MR scan of a phantom was initiated in MR5. During the phantom scan, the magnetic field strength was measured at locations just outside the MR5 entrance (Figure 4, Points A, B and C). After the phantom scan was completed, measurements inside the MR5 room at location D were made to determine the field variance. This test also provided data to assess the need for a Magnetic Active Cancellation System in the MR5 suite. The radiating loop (generating a 60 G field) was then moved just outside the north entrance doors of the MRI facility to measure attenuation along the MRI facility aisle. These measurements were used to estimate possible interference with any of the other scanners beyond MR5. After completion of the magnetic field testing the radiating loop was moved to inside the South wall of the PT facility to measure attenuation of the 2.4 m thick high-density concrete wall.

It should be pointed out that the 60 G field generated did not simulate all parameters in a Mevion system. Thus while the tests provided important information about the effect of an external time varying field on MR imaging at MR5, further tests were required with the 9TSM at full current and rotating to simulate the clinical environment in surrounding areas of the UHPTC.

2.2.3. Magnetic field measurements under time-varying 9T magnetic field

Upon installation of the Mevion S250PTS, several measurements were carried out to provide empirical measurements of the shielding performance with an AlphaLab Vector/Magnitude Gaussmeter (VGM). As the superconducting magnet current was gradually ramped up, magnetic flux was measured at 1000 Amp (field strength ~ 2T) and at full current of 1990 Amp (field strength ~9T) for different gantry angles and at several locations inside the accelerator vault, in the walkway, and inside the MR5 room. Note that direct correlation between the flux density and 9TSM field strength is not feasible because of various structures in the vicinity that affect the flux line characteristics. In an air environment the correlation is easily calculated, but with various metal structures having varying degrees of permeability, the complexity of the model would require data that is not available. The measurements reflect magnetic field variations that could produce interference to MRI scanning in MR5.

2.2.4. MR scanning under time-varying 9T magnetic field

Test MRI scans of phantoms were performed on MR5 with the S250PTS superconducting magnet at full current for three scenarios of S250 gantry position and movement. Baseline data without the S250 magnet were not obtained, but some measurements were compared to prior annual QA measurements taken prior to the S250 installation. The baseline case was the S250 gantry stationary in the 90° position, which results in the greatest distance between the cyclotron and the MRI scanner. Tests were repeated with the gantry stationary in the 0° position (closest to the MRI scanner) and with the gantry rotating at full clinical speed (6°/second). The phantom used for all tests was the factory-supplied body QC phantom (Siemens Healthcare, Erlangen, Germany), a spherical phantom with diameter 24 cm, filled with an ionic nickel solution and placed within an annular "body loader" filled with sodium chloride solution for electrical loading of the transmit coil.

For each of the three scenarios (representing possible cases for external magnetic field interference), several tests were carried out. The software Phantom Shim Check was performed, using an automated gradient echo field-mapping scan and automated analysis tool (Siemens Healthcare), to investigate any gross perturbation of the magnetic field within the MRI scanner. The Fat Saturation check was performed to identify induced magnetic field changes with clinical significance. Both of these checks are expected to be highly sensitive to the effect of an applied external magnetic field. A signal-to-noise ratio (SNR) test was performed using the integral receive body coil in three orthogonal planes.

Since a concern with external time-varying magnetic fields in MRI is effects that manifest at specific TR values, a series of gradient echo images and a series of spin echo planar (SE-EPI) images, each with varying TR and narrow receiver bandwidth, were performed to detect any pulse sequence-specific effects of the external magnetic fields from the S250PTS. The gradient echo and SE-EPI images were assessed for SNR changes and geometric distortion.

Gradient echo images were assessed for geometric distortion by measuring the phantom diameter along the horizontal and vertical axes. SE-EPI phantom images were assessed qualitatively for geometric distortion since this scan contains inherent geometric distortion at baseline that confounds the measurement. The parameters used in the MRI phantom testing are listed in Table 1.

© Cheng et al. Published by EJourPub.

Table 1: MR test scanning parameters used in each of 3 external magnetic field scenarios (gantry stationary in 0° and 90° positions and rotating at 6°/second).

Sequence Type	Bandwidth (Hz/pixel)	TR Values
Gradient Echo	60	20, 40, 80, 160, 320, 640
Spin Echo EPI	752	1000, 2000, 3000, 4000, 5000, 6000, 7000

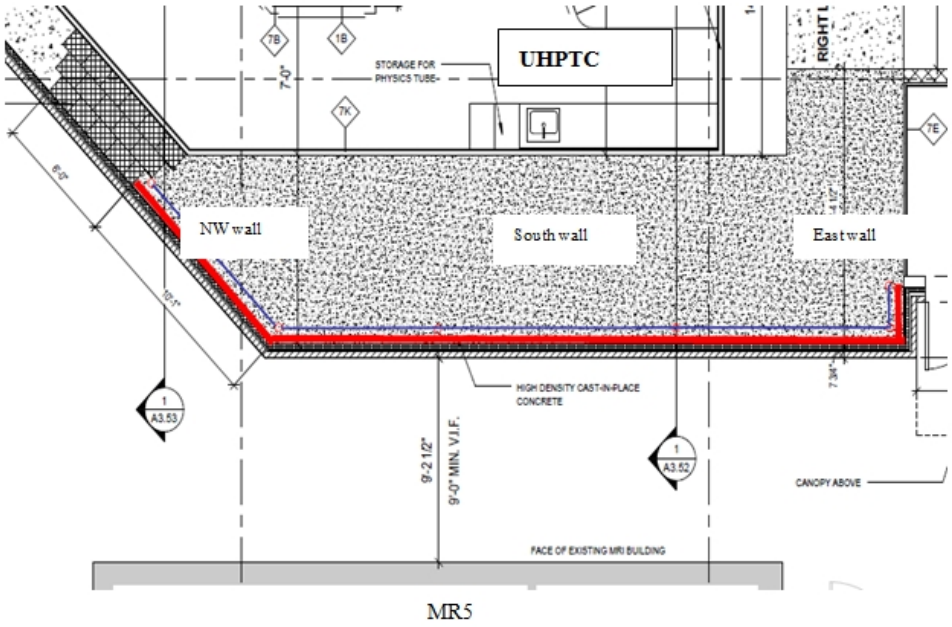

Figure 2: Design and construction of the RF shielding

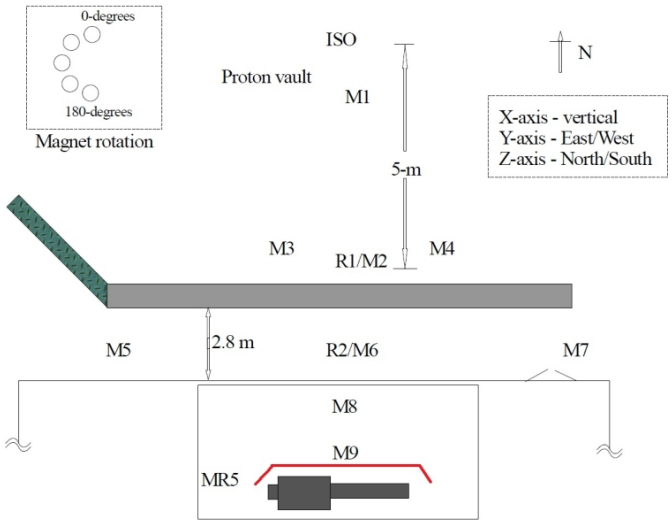

Figure 3: **Figure 3**: RF and magnetic field testing locations (not to scale). The points M1-M9 and R1-R3 are the magnetic field and RF

© Cheng et al. Published by EJourPub.

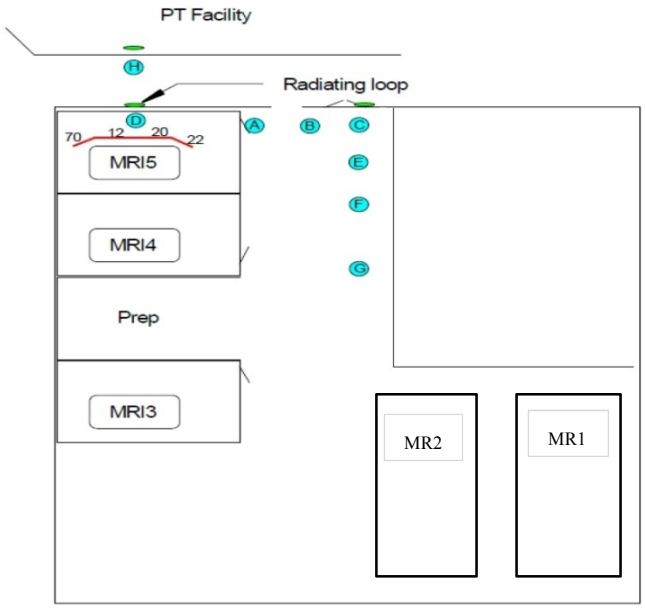

Figure 4: Magnetic field testing with a 60 G field. The measurement points are labeled A-H. The numbers along the red line in the sketch are field strength measurements (in Gauss) of the magnetic field from the MR5 magnet (no external interference was being generated during these measurements).

3. Results

3.1. Effect of RF on MR scanning

RF measurements inside the treatment vault at R1 show high level emissions. In the walkway at R2, no significant RF signal was detected at 120 MHz. The large difference between the signal strengths at R1 and R2 shown in Figure 5 is evidence of RF shielding effectiveness. The shielding provides 45-70 dB attenuation; the test was limited to measurements inside and outside of the vault wall, and the effects of MRI room wall and free space attenuation were not included in these measurements. With full power active RF (11 kW) and the proton therapy gantry rotated to various angles, no interference was reported on patient scanning throughout the testing. These results agreed with the very low level of RF signals measured at the equipment room door (R3) between MR1 and MR2 for different proton gantry angles.

3.2. Induced external magnetic fields in MRI area

The magnetic field strengths measured at locations A – H (see Figure 4) from the time-varying 60 G field are listed in Table 2. The 36.2 dB difference between points E and G is higher than attenuation in free space (which should be ~30 dB for that distance change) indicating that the magnetic field is somewhat shielded by the MRI facility construction. The magnetic field strength at H outside of the 2.4 m thick wall (the south wall) and the field strength at E which is 3 m from the radiating loop follow a power law of $1/r^{2.43}$ indicating that the high density concrete wall provides no significant shielding of the magnetic field. Note that measurement at point D in Table 2 was caused by the MR5 magnet within the room, and no time varying field component was detected.

Figure 6 below shows the change in the magnetic flux density at M1 (Figure 3) as the 9TSM was being ramped up slowly. The magnetic flux density remained relatively constant at 1 G from 300-1200 Amp and then increased rapidly at a rate of ~1.2 G/100 Amp.

Figure 7 shows the variation of magnetic flux density as a function of magnet angles at the different magnetic field testing points (as shown in Figure 3). As expected, the magnetic flux density at M1 (corresponds to the gantry isocenter) is higher than those at M2-M8. The magnetic flux density falls off by a factor of 4-6 between M1 and M2. However the magnetic flux density at M5 and M8 is only 1.3-1.6 times lower than that at M2. The variation of magnetic flux density with magnet angles remains relatively constant for M2-M8. At M8, a small effect due to the 9T magnetic field can still be detected. At M9, however, the magnetic field of the MR scanner dominates as indicated by the large constant values at M9.

© Cheng et al. Published by EJourPub.

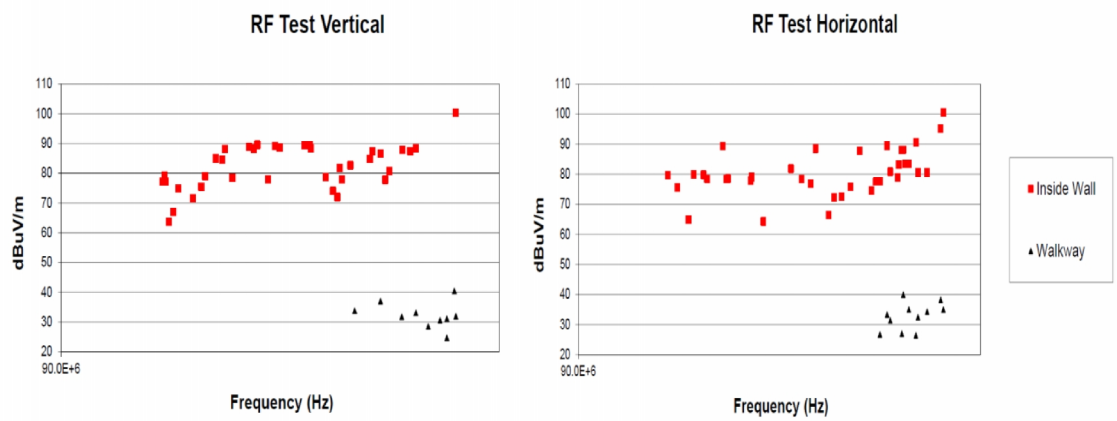

Figure 5: Sample results of RF measurement at R1 and R2 (Please see Figure 3). The 60dB reduction in RF signals at walkway location indicates the RF shielding design is effective. The RF frequency range of Mevion S250 is 90-133 MHz, which overlaps with that of the 3 Tesla MR scanners (MR1 and MR2).

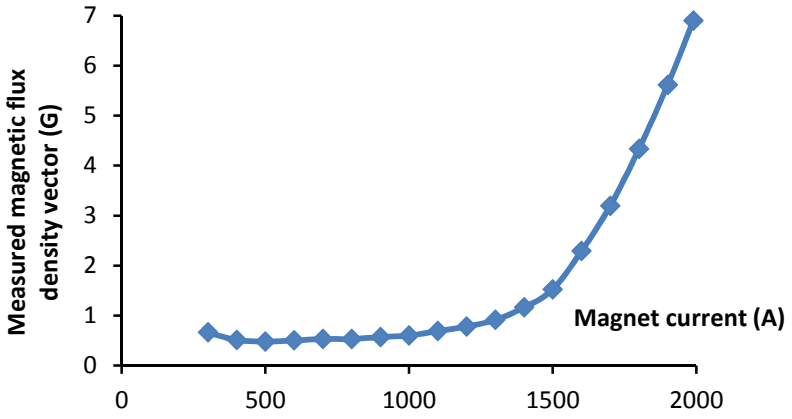

Figure 6: Measured magnetic flux density vector at M1 as function

Table 2: Measured magnetic field strengths at the different points as shown in Figure 4 due to a simulated time varying 60 G magnetic field placed outside of MR5.

Points of measurement	Location of points	Measured magnetic field strength (mG)
A	At MR5 closed door	2200
B	~ 1 m from MR5 door	900
C	~ 3 m from MR5 door	50
D	At MR5 north wall	2780
E	3 m from radiating loop	58
F	6 m from radiating loop	9.4
G	10 m from radiating loop	0.9
H	Outside south wall of vault, opposite radiating loop	100

© Cheng et al. Published by EJourPub.

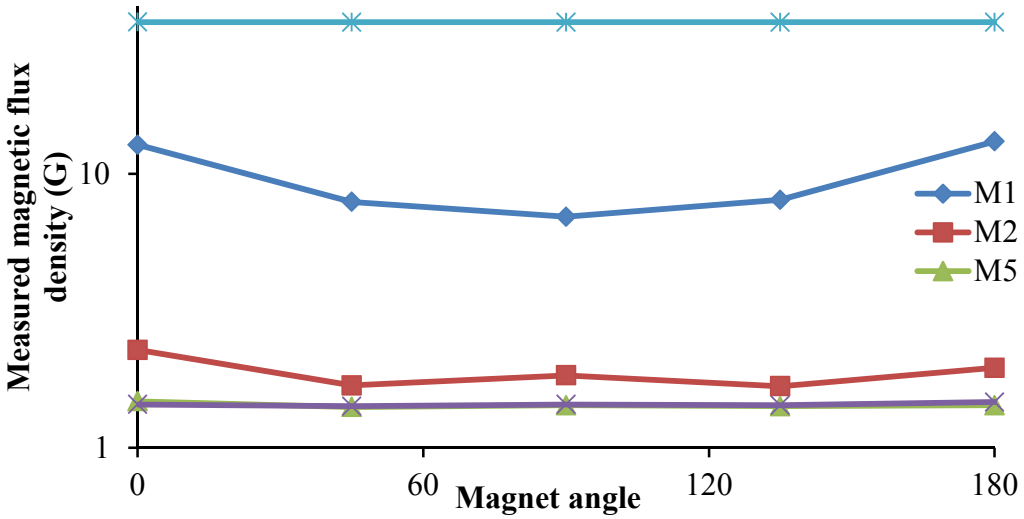

Figure 7: Measured magnetic flux density as a function of magnet angle at different points of interest. The effect of the 9T magnet field may still be seen at M8. The much higher readings at M9 are due to the MR magnet. The 9T field contribution is not detectable at this location.

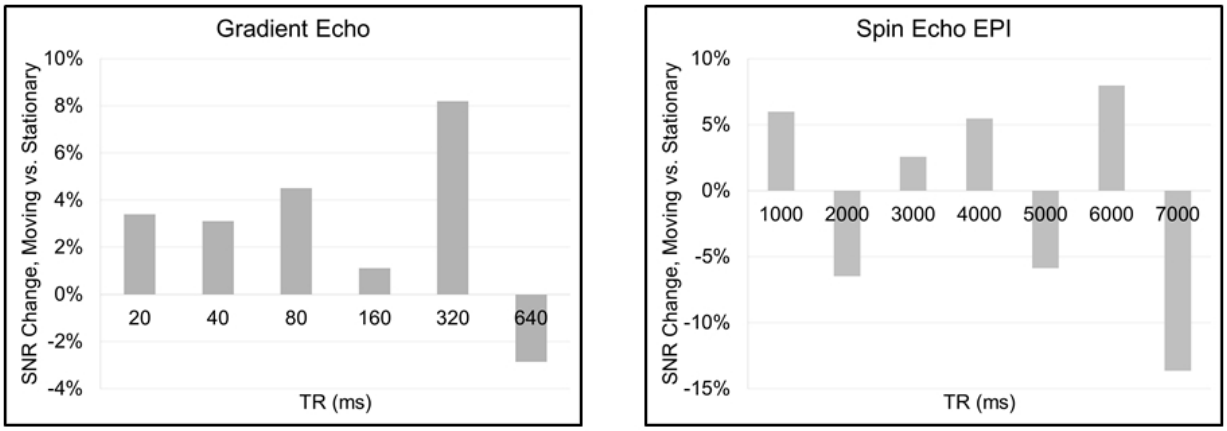

Figure 8: SNR changes at varying MRI scan TR values. Positive differences indicate higher SNR was measured for MRI scans performed while the S250PTS gantry was moving; negative differences indicate SNR was higher with the S250PTS gantry stationary.

3.3. Effect of external time-varying magnetic fields on MR scanning

The measured magnetic field inhomogeneity in the MRI scanner (MR5) varied by up to 6% across the S250PTS position/motion scenarios; all results were well within the factory specification provided by Siemens. The worst of the three measurements was 3.6% better than the results from the last annual QA survey (performed approximately three months earlier, before the S250PTS superconducting magnet was energized). This suggests that the presence of the external magnetic field does not significantly perturb the MRI scanner's magnetic field; the variations observed likely reflect typical inter-measurement variation rather than physical changes.

The MRI fat saturation test results showed variations of less than 10% from baseline across the S250PTS position/motion scenarios. All measured values conform to the Siemens factory specifications. The largest variations observed (-7% signal in the coronal plane and -10% signal in the sagittal plane) indicate improved, rather than degraded, fat suppression performance. There is no physical mechanism to explain improved fat suppression when an external magnetic field is applied to a highly homogeneous MRI magnetic field, so it is likely that these variations also represent normal inter-measurement variations rather than a physical effect due to the S250PTS. The MRI system SNR measurements exceeded factory minimum specifications and fluctuated by less than ± 1% from baseline across the S250PTS position/motion scenarios. The signal uniformity varied by less than ± 3% in the three principal image planes.

© Cheng et al. Published by EJourPub.

Gradient echo phantom images showed no significant geometric distortion. One measurement (Y-axis for the TR= 20 ms scan) varied by 1.7% between the S250PTS position and motion scenarios, and all other measurements fluctuated by less than 1%. There was no geometric distortion observed qualitatively during scanning. SNR measurements fluctuated by no more than 8% for the range of TR values scanned. While this variation is larger than that observed using the factory SNR checks (scanned using less sensitive spin echo techniques), the variations in SNR were both positive and negative, suggesting inter-measurement variation rather than degradation of the scan performance due to interference.

SE-EPI phantom scans showed no geometric distortion upon qualitative inspection aside from the inherent distortion observed at baseline. SNR measurements showed fluctuation at various TR values when comparing the cases of stationary and moving S250PTS gantry, ranging from the MRI SNR 8% higher to 14% lower for the moving gantry case.

The difference in SNR between the moving proton gantry and the stationary proton gantry is plotted against scan TR for the gradient echo and SE-EPI MRI tests in Figure 8.

4. Discussion

We have carried out RF measurements at an existing Mevion site (BJH) to aid the design of RF shielding for the proton facility at UH. We have also carried out several tests with a time-varying magnetic field and RF source (simulating the potential interference caused by the Mevion S250) to estimate their effects on MRI scanning in MR5 which is closest to the UHPTC. These tests showed that a Magnetic Active Compensation System is not necessary in this configuration since no MRI interference was detected throughout the testing. With the S250 magnet at full current and rotated to different angles, and with RF at full power, magnetic field strengths were measured at several locations of interests inside the proton vault and MR5. MR scanning of patients was being performed throughout the tests. We found that the operation of the Mevion proton accelerator S250 with full current (1990 Amp) to generate a 9T superconducting magnet and full RF power at 11 kW did not produce interference with MRI during patient scanning. Phantom scanning in MR5 using scan sequences expected to be sensitive to external magnetic field effects further demonstrated that MR scanning was not significantly affected by the operation of the nearby Mevion S250PTS.

To the best of our knowledge, this is the first report on the effects of a 9T magnetic field and 11 kW RF source to a nearby MR imaging facility. The results have two important implications. First, the compact Mevion S250 PTS provides a viable solution to proton therapy in an urban setting where real estate may be at a premium price and where other medical facilities may exist in vicinity, in particular facilities that operate strong magnetic fields for clinical or research activities. Second, radiation oncology facilities wishing to install proton therapy and MRI equipment (such as for MR simulators or MR-guided therapy systems) in the same facility can use the results and interference mitigation strategies presented herein to guide their site planning.

5. Conclusion

With careful planning on RF shielding and elaborate measurements on the effects of RF and magnetic field measurements, we have shown that the superconducting synchrocyclotron of Mevion S250 PTS provides a viable solution to proton therapy in an urban setting where real estate may be at a premium price and where other medical facilities which operate strong magnetic fields for clinical or research may already exist in vicinity.

Conflict of Interest

The authors (Cheng C-W, Ferguson S, Jordan D, Jesspeh F, Mansur D and Wessels B) received no financial support from the Mevion Medical Systems. Two of the authors (Johnson M and Bouchet L) are associated with the Mevion Medical Systems.

Funding

The measurements conducted at the Barnes Jewish Hospital in St. Louis, MO, on-site at the UHPTC as well at the MR suites were supported by a fund from the UH Proton Project.

Acknowledgement

The authors would like to thank the Barnes Jewish Hospital to allow access to the various locations at the hospital for the initial magnetic field and RF measurements. The authors would also like to thank the MR Department at University Hospitals Cleveland Medical Center to allow access to the various MR suites and other locations inside the building for the magnetic field and RF measurements. The authors would like to acknowledge Gilbane Construction Company and TKA Architects for assistance on custom designing RF shield in the south wall (under S Ferguson's direction).

References

1. Mevion S250 Subsystems I and II, Mevion Medical Systems Publication.
2. Soueid A, Teague EC, Murday J. Buildings for Advanced Technology: Chapter 8, EMI/RFI: Electromagnetic and RadioFrequency Interference. Part of the series Science Policy Reports. 2015: 93-114.
3. Jackson EF, Bronskill MJ, Drost DJ, *et al.*

© Cheng et al. Published by EJourPub.

Acceptance testing and quality assurance procedures for magnetic resonance imaging facilities. MR subcommittee Task Group I. AAPM Report 100, 2010.

© Cheng et al. Published by EJourPub.